

Rate Statistics in Cellular Downlink: PHY Rateless vs Adaptive Modulation and Coding

Amogh Rajanna *Member, IEEE*, and Carl P. Dettmann

Abstract

In this letter, we focus on rateless coded adaptive transmission in a cellular downlink. Based on a stochastic geometry model for the locations of BSs, we evaluate the meta-distribution of rate, i.e., the distribution of rate conditioned on the point process. An accurate approximation to the distribution of per-user rate is proposed and clearly shown to provide a good match to the simulation results. We quantify the gain in the per-user rate due to physical layer rateless codes relative to the fixed-rate adaptive modulation and coding.

Index Terms

Adaptive Modulation and Coding, Physical Layer Rateless Codes, Cellular Downlink, Stochastic Geometry and Meta-distribution.

I. INTRODUCTION

Modelling the locations of BSs and users by Poisson point processes (PPPs), it is shown in [1], [2] that an adaptive transmission scheme based on physical layer rateless codes is very robust in terms of providing enhanced coverage and rate relative to the one based on fixed-rate coding and power control. In [2], the metric used to compare the performance of adaptive transmission schemes is the typical user coverage probability and rate, which corresponds to the spatial average of users performance across the network. The meta-distribution of SIR is the distribution of coverage probability in the network conditioned on the point process [3] [4]. It gives a fine-grained statistical probe into the per-user performance in the network. For the first time in the literature, and using an accurate approximation, this letter characterizes the

The authors are with the School of Mathematics, University of Bristol, UK. Email: amogh.rajanna@ieee.org. The work was supported by the EPSRC grant EP/N002458/1 for the project *Spatially Embedded Networks*.

distribution of the per-user rate, i.e., rate conditioned on the point process in cellular downlink when rateless codes are used. The rate distribution provides a comprehensive probe into the performance enhancements due to rateless coding.

II. PERFORMANCE ANALYSIS

A. System Model

We consider a single tier cellular downlink in which the locations of BSs are modeled by a PPP $\Phi \triangleq \Phi_b \cup \{o\}$, where $\Phi_b = \{X_i\}$, $i = 1, 2, \dots$ is a homogeneous PPP of intensity λ [5]. A user served by a BS X_i is located uniformly at random within the Voronoi cell of X_i . The typical user is located within the *typical cell*, the Voronoi cell of the BS at origin. The distance between the typical user and the typical BS of Φ is D . Its approximate distribution is $D \sim \text{Rayleigh}(\sigma)$, with the scale parameter $\sigma = 1/\sqrt{2\pi\lambda}$ [1]. We consider a translated version of the PPP Φ so that the typical user is at the origin.

On the downlink, each BS transmits a K -bit packet to its user using a physical layer rateless code. Each BS transmits with constant power ρ . The channel is quasi-static flat fading affected by path loss. The interference power and SIR at the typical user based on the typical BS transmission are given by

$$I = \sum_{k \neq 0} \rho h_k |X_k|^{-\alpha} \quad (1)$$

$$\text{SIR} = \frac{\rho h D^{-\alpha}}{I}, \quad (2)$$

where h and h_k have $\text{Exp}(1)$ distribution.

Each packet transmission of K bits has a delay constraint of N channel uses. The time to decode a K -bit packet and thus, the packet transmission time T are given by

$$\hat{T} = \min \{t : K < t \cdot C\} \quad (3)$$

$$T = \min(N, \hat{T}), \quad (4)$$

where C is the achievable rate of the typical BS transmission and depends on the type of receiver used. Now, we focus on a framework introduced in [3] to study the network performance conditioned on the PPP Φ . In this letter, the two metrics used to quantify the performance of

rateless codes are the success probability and rate of K -bit packet transmission conditioned on Φ , defined as

$$P_s(N) \triangleq 1 - \mathbb{P}(\hat{T} > N \mid \Phi) \quad (5)$$

$$R_N \triangleq \frac{K P_s(N)}{\mathbb{E}[T \mid \Phi]}. \quad (6)$$

Both $P_s(N)$ and R_N depend on the distribution of \hat{T} conditioned on Φ . R_N in (6) is a random variable (RV). It quantifies the per-user rate achieved in a given PPP realization Φ .

From (4), the CCDF of T is $\mathbb{P}(T > t) = \mathbb{P}(\hat{T} > t)$, $t < N$. Plugging the expression for C in (3), we obtain

$$\mathbb{P}(\hat{T} > t) = \mathbb{P}(K/t \geq \log_2(1 + \text{SIR})) \quad (7)$$

$$P_s(t) \triangleq \mathbb{P}(\hat{T} \leq t \mid \Phi) = \mathbb{P}(\text{SIR} \geq \theta_t \mid \Phi), \quad (8)$$

where $\theta_t = 2^{K/t} - 1$.

In the following, we discuss the conditional packet transmission time distribution for two types of interference models. One type is the constant interference model and the second type is the time-varying interference model.

B. Constant Interference

Under the constant interference (CI) model, it is assumed that the interfering BSs are transmitting *continuously* to their users for the entire duration of the typical user reception time. The typical BS transmits a K -bit packet to the typical user and the performance under such a scenario is characterized below. Note that the CDF in (8) is a RV due to conditioning on Φ . A direct calculation of the distribution of $P_s(t)$ is infeasible. Below, we quantify the moments of $P_s(t)$ in (8).

Theorem 1. *The moments of the conditional CDF of the packet transmission time, $P_s(t)$ in (8), are given by*

$$M_n \triangleq \mathbb{E}[(P_s(t))^n] = \frac{1}{{}_2F_1([n, -\delta]; 1 - \delta; -\theta_t)}, \quad (9)$$

where ${}_2F_1([a, b]; c; z)$ is the Gauss hypergeometric function and $\delta = 2/\alpha$.

Proof: Note that

$$M_n = \mathbb{E}[(P_s(t))^n] = \mathbb{E}[(\mathbb{P}(\text{SIR} \geq \theta_t \mid \Phi))^n]. \quad (10)$$

An expression for the $\mathbb{E}[\cdot]$ in (10) for the SIR expression in (2) is given in [3, Theorem 2] for a fixed θ . ■

C. Time-varying Interference

Under the time-varying interference (TvI) model, we assume that the interfering BSs transmit only a K -bit packet to their user and become silent afterwards. Since the packet transmission time of each interfering BS is random, the interference at the typical user is time-varying. The time-averaged interference up to time t is given by [1]

$$\hat{I}(t) = \sum_{k \neq 0} \rho h_k |X_k|^{-\alpha} \min(1, T_k/t), \quad (11)$$

where T_k is the packet transmission time of BS X_k .

Assuming each user employs a nearest-neighbour decoder, the achievable rate at the typical user is given by

$$C(t) = \log_2(1 + \text{SIR}(t)), \quad (12)$$

where $\text{SIR}(t)$ is based on $\hat{I}(t)$ in (11) and obtained from (2) with $\hat{I}(t)$ replacing I . The packet transmission time distribution depends on the Laplace transform (LT) of the interference $\hat{I}(t)$. However, due to the fact that the marks T_k are correlated, it is infeasible to find the LT of $\hat{I}(t)$. For the sake of analysis, we consider an approximation termed independent thinning model (ITM) in which the correlated marks T_k are replaced by i.i.d. marks \bar{T}_k with a given CDF $F(\bar{t})$. The average interference up to time t under ITM is given by

$$\bar{I}(t) = \sum_{k \neq 0} \rho h_k |X_k|^{-\alpha} \min(1, \bar{T}_k/t). \quad (13)$$

Let $\bar{\eta}_k(t) = \min(1, \bar{T}_k/t)$. We just use $\bar{\eta}_k$ for simplicity. The corresponding achievable rate is obtained from (12) with $\bar{I}(t)$ in (13) replacing $\hat{I}(t)$. The analysis of the TvI model is based on the ITM assumption throughout the paper. The CDF of \hat{T} when conditioned on Φ under the ITM is given by

$$P_s(t) \triangleq \mathbb{P}(\hat{T} \leq t \mid \Phi) = \mathbb{P}\left(\frac{\rho h D^{-\alpha}}{\bar{I}(t)} \geq \theta_t \mid \Phi\right). \quad (14)$$

The moments of the RV $P_s(t)$ in (14) are quantified below.

Theorem 2. *The moments of the conditional CDF of the packet transmission time under the independent thinning model, $P_s(t)$ in (14), are bounded as*

$$M_n \triangleq \mathbb{E}[(P_s(t))^n] \geq \frac{1}{{}_2F_1([n, -\delta]; 1 - \delta; -\omega(t)\theta_t)} \quad (15)$$

$$\omega(t) = 1 - \frac{1}{t} \int_0^t F(x) dx \quad (16)$$

$$F(t) = \frac{1}{{}_2F_1([1, -\delta]; 1 - \delta; -\theta_t \min(1, \mu/t))} \quad (17)$$

$$\mu = \int_0^N (1 - {}_2F_1([1, \delta]; 1 + \delta; -\theta_t)) dt. \quad (18)$$

Proof: Note that $P_s(t)$ in (14) can be written as

$$\begin{aligned} P_s(t) &= \mathbb{P}\left(h \geq \theta_t D^\alpha \sum_{k \neq 0} h_k |X_k|^{-\alpha} \bar{\eta}_k \mid \Phi\right) \\ &= \prod_{k \neq 0} \mathbb{E}_{\bar{\eta}} \left[\frac{1}{1 + \theta_t (D/|X_k|)^\alpha \bar{\eta}_k} \right] \end{aligned} \quad (19)$$

$$\stackrel{(a)}{\geq} \prod \frac{1}{1 + \theta_t (D/|X_k|)^\alpha \mathbb{E}[\bar{\eta}_k]}, \quad (20)$$

where (a) follows by applying Jensen's inequality for convex functions in (19). Letting $\bar{\theta}_t = \theta_t \mathbb{E}[\bar{\eta}_k]$, we get

$$M_n = \mathbb{E}[(P_s(t))^n] \geq \mathbb{E}\left[\prod \frac{1}{(1 + \bar{\theta}_t (D/|X_k|)^\alpha)^n}\right] \quad (21)$$

$$\stackrel{(a)}{=} \mathbb{E}\left[\exp\left(-\pi\lambda \int_D^\infty \left(1 - \frac{1}{(1 + \bar{\theta}_t (D/v)^\alpha)^n}\right) dv^2\right)\right]$$

$$\stackrel{(b)}{=} \mathbb{E}\left[\exp\left(-\pi\lambda D^2 \underbrace{\delta \bar{\theta}_t^\delta \int_0^{\bar{\theta}_t} \left(1 - \frac{1}{(1 + y)^n}\right) \frac{dy}{y^{1+\delta}}}_{H(\bar{\theta}_t)}\right)\right]$$

$$\stackrel{(c)}{=} \frac{1}{1 + H(\bar{\theta}_t)} = \frac{1}{{}_2F_1([n, -\delta]; 1 - \delta; -\theta_t \mathbb{E}[\bar{\eta}])}, \quad (22)$$

where (a) follows from the PGFL of the uniform PPP Φ_b , (b) is obtained from a substitution $y = \bar{\theta}_t (D/v)^\alpha$ and the $\mathbb{E}[\cdot]$ operation w.r.t D leads to (c). The function $H(\bar{\theta}_t)$ can be expressed as in (22). The relation between $\mathbb{E}[\bar{\eta}]$ in (22) and $\omega(t)$ in (15) is derived in [2, Theorem 1]. ■

Note that the above function $H(\bar{\theta}_t)$ was based on the lower bound in (20). The corresponding function that can be obtained based on the exact expression in (19) is given below.

$$G(\theta_t) = \delta \theta_t^\delta \int_0^{\theta_t} \left(1 - \left(\mathbb{E} \left[\frac{1}{1 + \bar{\eta} y} \right] \right)^n \right) \frac{dy}{y^{1+\delta}} \quad (23)$$

$$M_n = \frac{1}{1 + G(\theta_t)} \geq \frac{1}{1 + H(\bar{\theta}_t)} \triangleq \tilde{M}_n. \quad (24)$$

$G(\theta_t)$ in (23) can be further written out in closed form. However, it is not feasible to provide a simple expression for $G(\theta_t)$ in terms of the hypergeometric function similar to $H(\bar{\theta}_t)$. Hence, we work with the bound $H(\bar{\theta}_t)$ for tractability. From now onwards, we just use the tractable approximation \tilde{M}_n defined in (24) instead of M_n . Based on the moments \tilde{M}_n , an expression for the CDF (or its bounds) of the RV $P_s(t)$ in (14) can be written out in closed form [3]. However, since $P_s(t)$ is supported on the interval $[0,1]$, the beta distribution will be useful. Since $\mathbb{E}[\bar{\eta}] = 1$ and hence $\bar{\theta}_t = \theta_t$ for the CI model, it can be regarded as a special case of the TvI model.

III. DISTRIBUTION APPROXIMATIONS

A. Beta Approximation of $P_s(t)$ for CI and TvI models

The PDF of beta-approximated $P_s(t)$ is given by

$$f(x) = \frac{x^{\bar{\gamma}-1} (1-x)^{\beta-1}}{B(\bar{\gamma}, \beta)}, \quad x \in [0, 1], \quad (25)$$

where $B(a, b) = \int_0^1 x^{a-1} (1-x)^{b-1} dx$ is the beta function and $\bar{\gamma} = \gamma\beta/(1-\gamma)$, with γ and β related to the moments of $P_s(t)$ as [3]

$$\gamma = \tilde{M}_1; \quad \beta = \frac{(\gamma - \tilde{M}_2)(1-\gamma)}{\tilde{M}_2 - \gamma^2}. \quad (26)$$

Note that both the parameters γ and β are functions of t .

B. R_N Distribution Approximation for CI and TvI models

From (6), the distribution of R_N can be obtained from the PDF of $P_s(N)$ given in (25) and (26) with $t = N$ and also, the distribution of $\mathbb{E}[T | \Phi]$. Let

$$T_\phi \triangleq \mathbb{E}[T | \Phi] = \int_0^N \left(1 - \mathbb{P}(\hat{T} \leq t | \Phi) \right) dt. \quad (27)$$

Now, the CCDF of rate R_N in (6) is given by

$$\begin{aligned} \mathbb{P}(R_N > r) &= \mathbb{E} \left[\mathbb{P} \left(P_s(N) > \frac{r T_\phi}{K} \middle| T_\phi \right) \right] \\ &= \frac{\mathbb{E} [\bar{B}(r T_\phi / K, \bar{\gamma}, \beta)]}{B(\bar{\gamma}, \beta)}, \end{aligned} \quad (28)$$

where $\bar{B}(a, b, c) = \int_a^1 y^{b-1} (1-y)^{c-1} dy$ is the upper incomplete beta function. To evaluate (28), the distribution of T_ϕ in (27) is very critical. We first obtain the moments of T_ϕ .

From (27), the first two moments of T_ϕ are given by

$$\nu_1 = \mathbb{E}[T_\phi] = N - \int_0^N \tilde{M}_1(t) dt \quad (29)$$

$$\begin{aligned} \nu_2 = \mathbb{E}[T_\phi^2] &= \mathbb{E}\left[\left(N - \int_0^N P_s(t) dt\right)^2\right] \\ &\stackrel{(a)}{=} N(2\nu_1 - N) + \mathbb{E}\left[\left(\int_0^N P_s(t) dt\right)^2\right], \end{aligned} \quad (30)$$

where in (a), the second term is given below.

$$\begin{aligned} \mathbb{E}\left[\left(\int_0^N P_s(t) dt\right)^2\right] &= \mathbb{E}\left[\int_0^N P_s(t) dt \int_0^N P_s(u) du\right] \\ &= \int_0^N \int_0^N \mathbb{E}[P_s(t)P_s(u)] dt du \\ &\stackrel{(b)}{=} \int_0^N \int_0^N \frac{1}{1 + J(\bar{\theta}_t, \bar{\theta}_u)} dt du, \end{aligned} \quad (31)$$

where (b) is obtained based on the following steps.

$$\mathbb{E}[P_s(t)P_s(u)] = \frac{1}{1 + J(\bar{\theta}_t, \bar{\theta}_u)} \quad (32)$$

$$J(\bar{\theta}_t, \bar{\theta}_u) = \delta \int_0^1 \left[1 - \frac{1}{(1 + \bar{\theta}_t y)(1 + \bar{\theta}_u y)}\right] \frac{dy}{y^{1+\delta}}, \quad (33)$$

where $\bar{\theta}_t = \theta_t \mathbb{E}[\bar{\eta}]$ and $\bar{\theta}_u = \theta_u \mathbb{E}[\bar{\eta}]$. The result in (32) and (33) is derived using steps similar to that in the proof of Theorem 2. The $P_s(t)$ expression is given in (19) and (20). The $\mathbb{E}[\cdot]$ in (32) is computed using steps similar to (21)-(22), with the exception that $J(\bar{\theta}_t, \bar{\theta}_u)$ is the corresponding function instead of $H(\bar{\theta}_t)$. Using (31) and (33), the second moment ν_2 in (30) can be computed. For the CI model, the moment expressions are exact. However for the TvI model, the moment expressions are approximate since they are based on the tractable approximation of $P_s(t)$ in (20). It is not feasible to express T_ϕ moments in closed form based on the exact $P_s(t)$ in (19). The PDF of $T_\phi \in [0, N]$ is approximated by a known distribution, whose parameters are expressed in terms of the moments of T_ϕ .

Beta distribution has been used widely to approximate the distribution of a RV with finite support. Hence, we propose to model T_ϕ/N as a beta distributed RV. The first two moments of T_ϕ/N are given by

$$\kappa_1 = \frac{\nu_1}{N}; \quad \kappa_2 = \frac{\nu_2}{N^2}. \quad (34)$$

Now, the two parameters $\bar{\kappa}$ and ϑ of the beta distribution for the RV T_ϕ/N are given by

$$\vartheta = \frac{(\kappa_1 - \kappa_2)(1 - \kappa_1)}{\kappa_2 - \kappa_1^2}; \quad \bar{\kappa} = \frac{\kappa_1 \vartheta}{1 - \kappa_1}. \quad (35)$$

The PDF of T_ϕ/N is similar in form to (25) except for the parameters $\bar{\kappa}$ and ϑ . Below, we summarize the main result of the preceding discussion.

Theorem 3. *The CCDF of the per-user rate R_N in (6) is given by*

$$\mathbb{P}(R_N > r) = \int_0^1 \frac{\bar{B}(rNy/K, \bar{\gamma}, \beta)}{B(\bar{\gamma}, \beta)} \frac{y^{\bar{\kappa}-1}(1-y)^{\vartheta-1}}{B(\bar{\kappa}, \vartheta)} dy. \quad (36)$$

C. Fixed-Rate Coding

For fixed-rate coding, the per-user rate is defined as

$$R_N \triangleq \frac{K}{N} \mathbb{P}(\text{SIR} > 2^{K/N} - 1 \mid \Phi). \quad (37)$$

The CCDF of the rate R_N is given by

$$\mathbb{P}(R_N > r) = \frac{\bar{B}(rN/K, \bar{\gamma}, \beta)}{B(\bar{\gamma}, \beta)}. \quad (38)$$

In the expression for parameters $\bar{\gamma}$ and β as per (26), the moments M_n given in (9) are used.

D. Fixed-rate Adaptive Modulation and Coding

Adaptive modulation and coding (AMC) is a scheme used in current 4G networks to adapt the rate to channel conditions [6]–[8]. AMC chooses a fixed-rate code and its code rate to most closely match the channel conditions. The preceding discussions in the current paper focused on rateless codes are also applicable to the case of AMC with one important change. For the rateless case, the packet time $t \in \mathbb{N}$ whereas for the AMC case, the resolution changes to $t = \{N_i\}$, where N_i is the number of parity symbols for the AMC index i .

IV. NUMERICAL RESULTS

In this section, numerical results showing the efficacy of the proposed per-user performance analysis are presented. For the network simulation, the following parameters were chosen: $\lambda = 1$ and $K = 75$. In Fig. 1, a plot of the CCDF of the per-user rate R_N is shown for a cellular network at $\alpha = 3$ and $N = 200$. The focus is on comparing three types of transmission schemes, i.e., fixed-rate coding based on (38), AMC as described in Section III-D and the rateless scheme as per (36). Note that the performance of AMC is based on simulation only. In terms of matching the

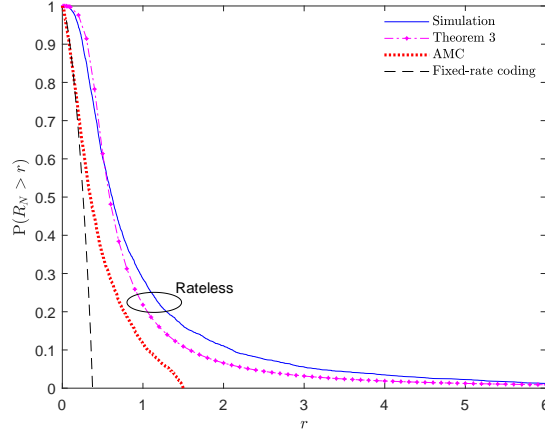


Fig. 1. The CCDF of the per-user rate R_N in (6) in a cellular downlink with $\lambda = 1$, $\alpha = 3$ and $N = 200$. The rateless coding curve is based on (36), while the fixed-rate coding curve is based on (38). For rateless coding, the curve is based on the time-varying interference model.

rate to the instantaneous channel conditions, fixed-rate coding has poor efficiency and rateless coding has high efficiency with AMC performance lying in between the two schemes. High efficiency of rateless coding is captured by the term $\mathbb{E}[T | \Phi]$ in the expression for R_N in (6). For fixed rate coding, the packet time is fixed to N . As noted in Section III-D, AMC is also based on fixed-rate codes and thus, the packet time does not change with a finer resolution as compared to the case for rateless coding.

Fig. 2 shows a plot of the CCDF of the per-user rate R_N for a cellular downlink at $\alpha = 4$ and $N = 100$. For AMC, the CCDF curve decays to zero at a rate of $r = 3$. For rateless coding, the CCDF at $r = 3$ is 0.15. Since rateless codes have robust adaptivity to the instantaneous channel conditions, the scheme yields much higher per-user rates relative to the AMC. These higher per-user rates for the rateless scheme have implications on the energy-efficiency of the BS-UE links and also, the congestion, QoS and end-to-end delay in the network. The AMC and rateless scheme have their implementation differences. AMC relies on pre-determined codeword lengths whereas the rateless scheme does not.

Enhancing the accuracy of the analysis: In Section III-B, the key ingredients in obtaining a distribution approximation for the per-user rate R_N were the moments and distribution of T_ϕ . Currently, we have restricted ourselves to the first two moments of T_ϕ . It is expected that using the three moments of T_ϕ leads to a better approximation of its distribution and thus, the same for

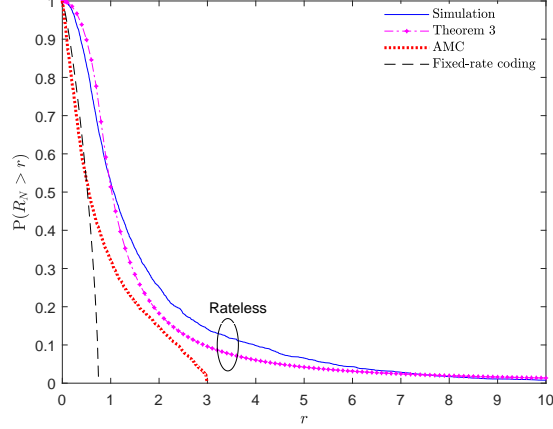


Fig. 2. The CCDF of the per-user rate R_N in (6) in a cellular downlink with $\lambda = 1$, $\alpha = 4$ and $N = 100$.

R_N distribution. However due to space limitations, we have not considered such an approach.

V. CONCLUSION

In this letter, we characterize the per-user performance of cellular downlink when physical layer rateless codes are used for adaptive transmission. The BS locations are modeled by a Poisson point process. Performance of rateless codes was presented under both the constant and time-varying interference models, respectively. Accurate approximations to the distribution of the per-user coverage probability and transmission rate are derived. The advantages of rateless codes are clearly illustrated by comparing their performance to fixed-rate based adaptive modulation and coding.

REFERENCES

- [1] A. Rajanna and M. Haenggi, “Enhanced Cellular Coverage and Throughput Using Rateless Codes,” *IEEE Transactions on Communications*, vol. 65, no. 5, pp. 1899–1912, May 2017.
- [2] A. Rajanna and C. Dettmann, “Adaptive Transmission in Cellular Networks: Do Physical Layer Rateless Codes Supersede Power Control?” *IEEE Transactions on Wireless Communications*, April 2018, <https://arxiv.org/abs/1804.10445>.
- [3] M. Haenggi, “The Meta Distribution of the SIR in Poisson Bipolar and Cellular Networks,” *IEEE Transactions on Wireless Communications*, vol. 15, no. 4, pp. 2577–2589, Apr 2016.
- [4] C. P. Dettmann and O. Georgiou, “Isolation Statistics in Temporal Spatial Networks,” *EPL*, vol. 119, no. 28002, July 2017.
- [5] H. ElSawy, A. Sultan-Salem, M. Alouini, and M. Z. Win, “Modeling and Analysis of Cellular Networks Using Stochastic Geometry: A Tutorial,” *IEEE Communications Surveys Tutorials*, vol. 19, no. 1, pp. 167–203, First Quarter 2017.
- [6] A. J. Goldsmith and S.-G. Chua, “Adaptive Coded Modulation for Fading Channels,” *IEEE Transactions on Communications*, vol. 46, no. 5, pp. 595–602, May 1998.

- [7] A. Ghosh, J. Zhang, J. Andrews, and R. Muhamed, *Fundamentals of LTE*, 1st ed. Prentice Hall, 2011.
- [8] G. Caire and K. R. Kumar, "Information Theoretic Foundations of Adaptive Coded Modulation," *Proceedings of the IEEE*, vol. 95, no. 12, pp. 2274–2298, Dec 2007.